Available online at www.sciencedirect.com
SCIENCE DIRECT
Journal of Power Sources 156 (2006) 1–7
JOURNAL OF POWER SOURCES
www.elsevier.com/locate/jpowsour

Bipolar concept for alkaline fuel cells

E. Gülzow *, M. Schulze, U. Gerke

Deutsches Zentrum für Luft- und Raumfahrt e.V., Institut für Technische Thermodynamik, Pfaffenwaldring 38-40, D-70569 Stuttgart, Germany

Available online 3 February 2006

Abstract

Alkaline fuel cell stacks are mostly build in monopolar configuration of the cells. At the German Aerospace Center a bipolar plate for alkaline fuel cells has been developed and characterized in a short stack. As a consequence of the sealing concept of the stack two different bipolar plate types are needed. Therefore, the number of cells can only vary by 2 if the end plates are not changed. The single cell as well as the short stack is characterized by various methods, e.g. *V–i* characteristics, electrochemical impedance spectroscopy (EIS).

As a result of the specific electrodes used the differential pressure between electrolyte and gas phase is limited to a few 10 mbar. At higher differential pressures gas crossover through the electrodes and electrolyte takes place with the result that the electrolyte may flood the flow fields. In contrast to PEFC, electrode supported by a metal net as conductor and mechanical support can be used in the AFC. Therefore, the structure of the flow field can be quite simple, this means flow fields with channels with large width and depth are possible. Consequently, the pressure loss over the flow field is very low. The single cell as well as the short stack was operated at overpressures of a few 10 mbar. The AFC can be operated without a compression but with a simple fan.

The developed cell design is also used for the characterization of the fuel cell components like electrodes and diaphragms. The test facility for the single cell and for the stack is fully computer controlled and allows the variation of the operation conditions, e.g. flow of the electrolyte, hydrogen flow, oxygen or air flow and cell temperature.

Keywords: Alkaline fuel cells; Bipolar cell; Low pressure

1. Introduction

Alkaline fuel cells (AFC) are an interesting alternative to polymer electrolyte membrane fuel cells (PEFC). AFCs have some advantages and disadvantages compared with polymer electrolyte fuel cells (PEFCs). Inexpensive nickel can be used as catalyst at the anodes and silver may be used as cathode catalyst. Therefore expensive precious-metal catalysts can be avoided. In addition, liquid alkaline solution is used as electrolyte; therefore, no expensive polymer membrane as electrolyte is necessary. The use of inexpensive materials for catalyst and electrolytes in AFC corresponds to a cost advantages in comparison to PEFCs. Considering only the costs of the materials, the AFC has a much higher potential for the commercialization of fuel cells.

The advantages of AFC are not limited to the cheaper materials, AFC has also advantages in the system engineering because no humidification of reactant gases is required for AFC operation, which is a significant problem of the present PEFCs. Furthermore, the liquid electrolyte may enable a simple cooling of the stack. Often, the liquid electrolyte is seen as a significant disadvantage because AFCs need an additional circulation system for the electrolyte. However, a similar circulation for liquids is also needed for high power density PEFC systems for the cooling of the stack. The electrolyte circulation in AFC may be more expensive because of the higher corrosivity of the electrolyte compared with water of other cooling media in the PEFC. A disadvantage of the AFC is that the alkaline solution must be reconcentrated during long-term operation. But this may be implemented into the system much easier compared to the complex water management in a PEFC.

Low temperature fuel cells represent an important element in pollution-free energy supply for mobile applications. It is a commonly opinion that carbon dioxide intolerance is the most important disadvantage of air-operated alkaline fuel cells [1,2]. This was one of the reasons that in the beginning of the 1990s the activities in alkaline fuel cell research were terminated or drastically reduced in most companies. As a consequence, also the financial support in the research institutes decreased [3].

* Corresponding author.
E-mail address: Erich.Guelzow@dlr.de (E. Gülzow).

0378-7753/$ – see front matter © 2005 Elsevier B.V. All rights reserved.
doi:10.1016/j.jpowsour.2005.08.032

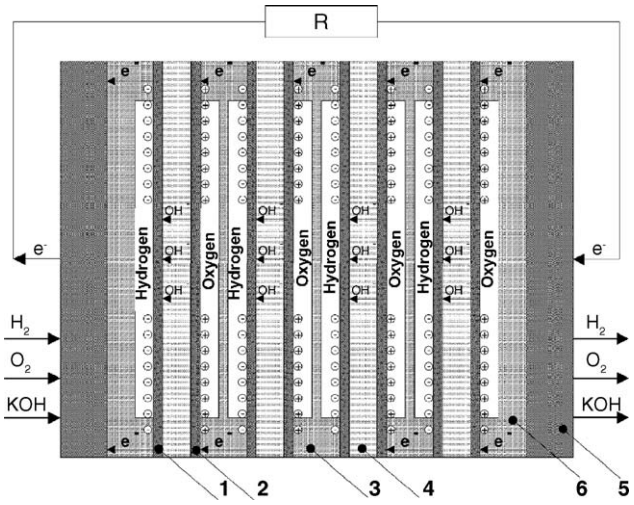

Fig. 1. Scheme of an alkaline fuel cell in bipolar configuration: (1) anode, (2) cathode, (3) bipolar plate, (4) electrolyte with spacer (diaphragm), (5) end plate, and (6) monopolar plate.

Thus, alkaline technology is commonly not considered in mobile fuel cell applications. In contrast to this view, in more recent publications a carbon dioxide tolerance of AFC was found [4–6].

The durability of fuel cells is a deciding factor for their commercialization. The degradation of fuel cell components is investigated with increasing activities mainly focussed on PEFC [7–18]. For alkaline fuel cells several studies of degradation processes exist [5,19–30]. These studies are focussed on the electrodes because the liquid electrolyte in AFCs can be easily exchanged and thereby renewed. The archived and reported life time of both fuel cell systems are similar. An advantage of the alkaline is that the degradation processes are better understood than in PEFC. Therefore, it seems more probable to solve the degradation problems for AFC in a short space of time.

2. Stack and test equipment

AFC stacks are frequently realized with an monopolar concept whereby the single cells are external connected. For PEFC, the bipolar configuration is commonly used, and the monopolar concept is only used in some specific low-power applications. In the work presented here a AFC stack in bipolar configuration was realized. The AFC stack should be operated at near ambient pressure. Another consideration in the stack design was that it should be suitable for component tests. Therefore the stack must be dismountable which excludes the common gluing of the stack and requires a suitable sealing concept.

The constructed stack consists of two end plates, the bipolar plates, the electrodes, the diaphragms and the sealings. First the stack was tested with just one cell to measure the dependence on pressure differentials in a simple set-up. In the following the stack was equipped with three cells. As mentioned before, due to the design of the stack, the stack can only be operated with an odd number of cells. Fig. 1 shows a scheme of the AFC stack. The end plates integrate the connections for the gas supply and the electrolyte circulation as well as for the electrical cables. In addition they have the function to distribute the contact pressure over the total area of the cells. The monopolar plates are for the first and last cell. The bipolar plates have the function of the distribution of the gases in the each cell by using the flow fields and to each cell by internal manifolding. Due to the higher thickness of the typical used AFC electrodes and an resulting higher gas diffusion in the electrodes the complexity for optimizing the flow fields in AFC is significant lower than for PEFCs. The diaphragms are needed to avoid the direct contact of the electrodes leading to a short circuit. Various diaphragms were tested in the stack.

Table 1
Used diaphragm materials

Name	Material	Thickness	Pore size (μm)
PE plates	Polyethylene, sintered	1–3 mm	125–175
PP non-woven material	Polypropylene	2–3 mm	–
Celgard 3401	Polypropylene plate	25 μm	0.117

3. Materials and used characterization methods

The bipolar plates, end plates and monopolar plates are manufactured from stainless steel. Although the stainless steel (X2CrNiMo18-14-3) has a sufficient stability against corrosion, the metallic components were electrochemical gold coated. In addition, the gold coating has a positive influence for the contact resistances.

As sealing material Ethylene–Propylene–Dien–Kautschuk (EPDM) was used, which can resist the alkaline solution. The EPDM sealings were cut by a water jet and two different thicknesses, 1.5 and 3.0 mm, were tested in the stack. Using this material the investigated stack was completely sealed. No KOH leakage was observed with exception of the PTFE fittings connecting the stack with the external electrolyte circuit.

As diaphragms sintered, porous polyethylene (PE) plates, polypropylene as non-woven material and a polypropylene plate with micro pores (Celgard 3401) were used. The characters of the diaphragm materials are listed in Table 1. As electrolyte 30% KOH solution was used.

As electrodes three different combinations were tested: electrodes with platinum catalyst from E-TEK were used as anodes as well as cathodes although these electrodes were developed for PEFC applications. The second investigated electrode combination was a E-TEK electrode as anode and a silver gas diffusion electrode as cathode; the third combination was a gas diffusion electrode with nickel as catalyst and the silver electrodes. The nickel and the silver electrodes are significant cheaper than the platinum electrodes, so they are preferred catalysts materials for commercial stacks. However they require an activation procedure [26]. In addition, the nickel and silver electrodes are not complete stable against at high loads because the oxidation state of the nickel can be irreversibly changed. Therefore, for the testing of the stack concept and as reference the use of platinum electrodes are helpful.

The assembled short stack with three cells is shown in Fig. 2. The stack was characterized electrochemically by recording

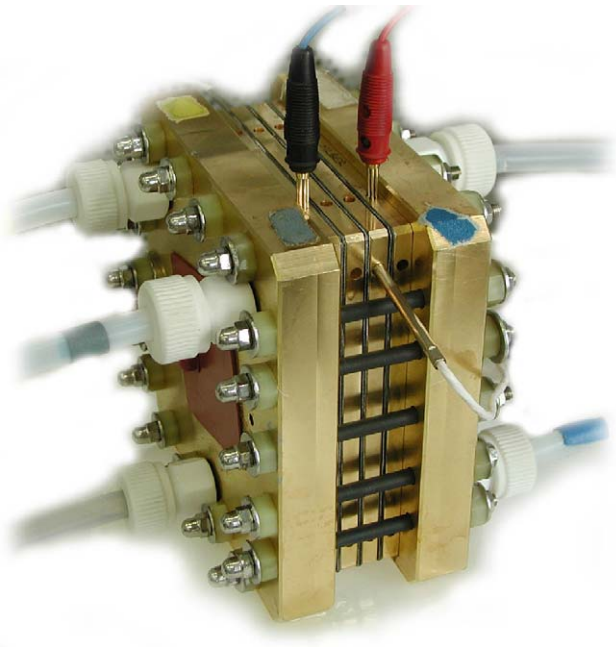

Fig. 2. AFC stack with three cells in bipolar configuration with connected supplies for gases and electrolyte, temperature sensor, heat pads and electrical contacts.

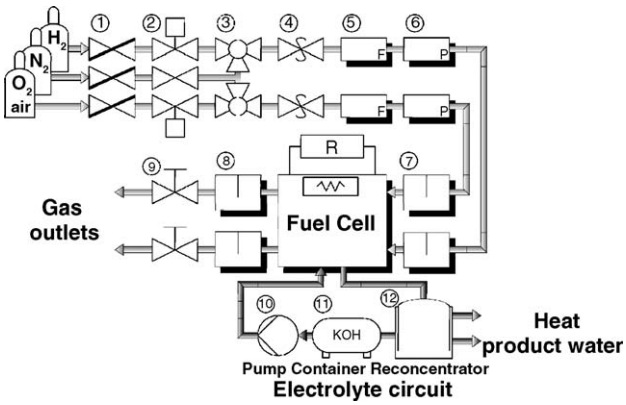

Fig. 3. Scheme of the AFC test facility.

V–i curves and by electrochemical impedance spectroscopy. During the measurement of the *V–i* curves each single cell voltage as well as the stack voltage was recorded. The electrochemical impedance spectroscopy was performed with an IM6 system from Zahner elektrik. The electrochemical measurements were performed to investigate the various diaphragms as well as the various electrode combinations. In addition, the influence of the temperature and the pressures of the media in the stack was investigated. The single cell voltages were recorded in order to determine the variation over the stack.

The tests were performed in a test facility controlled by a programmable logic controller (PLC), which allows the data acquisition of all operation parameters and the voltage of each cell as well as the controlling of each operation parameter like pressures, flow rates of the gases and the electrolyte as well as the stack temperature and electrical loading.

The scheme of a complete AFC system is displayed in Fig. 3 with exception of the reconcentrator for the electrolyte. The test facility in which the AFC system is installed is shown in Fig. 4.

4. Results

The internal resistance of the cell depends on the thickness of the electrolyte film between the electrodes. Other related factors affecting the conductivity are the diaphragms which determine the distance between the electrodes, the concentration of the electrolyte, and the average length of the electrolyte paths. The resistance of the electrolyte for the various diaphragms are determined by EIS. The measured resistance for the electrolyte for the various diaphragms are listed in Table 2. It is well known that the resistance of the electrolyte decreases with increasing temperature.

The measured resistance shows that the electrolyte-filled nonwoven polypropylene has the best conductivity. The specific resistance is nearly the same as for the free electrolyte. In contrast the resistance of the electrolyte-filled polyethylene plates is approximately four times higher. The microporous polypropylene material (Celgard) exhibits the highest specific resistance of the material, however, due to the low thickness of only 25 μm the total resistance is relative low. The Celgard diaphragm has the advantage that the pressure stability of the electrodes are enhanced.

Also various combinations of electrodes were characterized in the stack as described above. The *V–i* curves measured for various combinations of electrodes are shown in Fig. 5. The combination of a nickel electrodes as anodes and silver electrodes as cathodes shows the highest performance. Interestingly, the electrochemical performance of the stack decrease when substituting the nickel electrodes by platinum electrodes. This is especially evident at higher current densities. It has to be considered that in contrast to the nickel anodes the platinum electrodes are optimized for PEFC application. Therefore, the formation of the three phase zone between the liquid electrolyte, the gas phases and the catalyst surface may be inferior in the case of the platinum electrodes. Furthermore, the nickel electrodes are bulk unsupported catalysts and not carbon supported catalysts as in the case of the platinum electrodes. Therefore it is expected that the liquid electrolyte can contact most of the contiguous metal surface by surface films whereas for the carbon-supported catalysts the active area is reduced.

The substitution of the silver electrodes by platinum electrodes results in a further decrease of the electrochemical performance. This may also be explained by the better suitability of the silver electrodes to the requirements of the AFC. In addition the higher electrochemical activity of the silver catalysts for the oxygen reduction compared to the platinum catalyst should be taken into consideration.

The temperature of the system influences the electrochemical performance of the fuel cell not only by the well-known dependence of electrolyte resistance on temperature, but also by the acceleration of reaction kinetics with increasing temperature. In

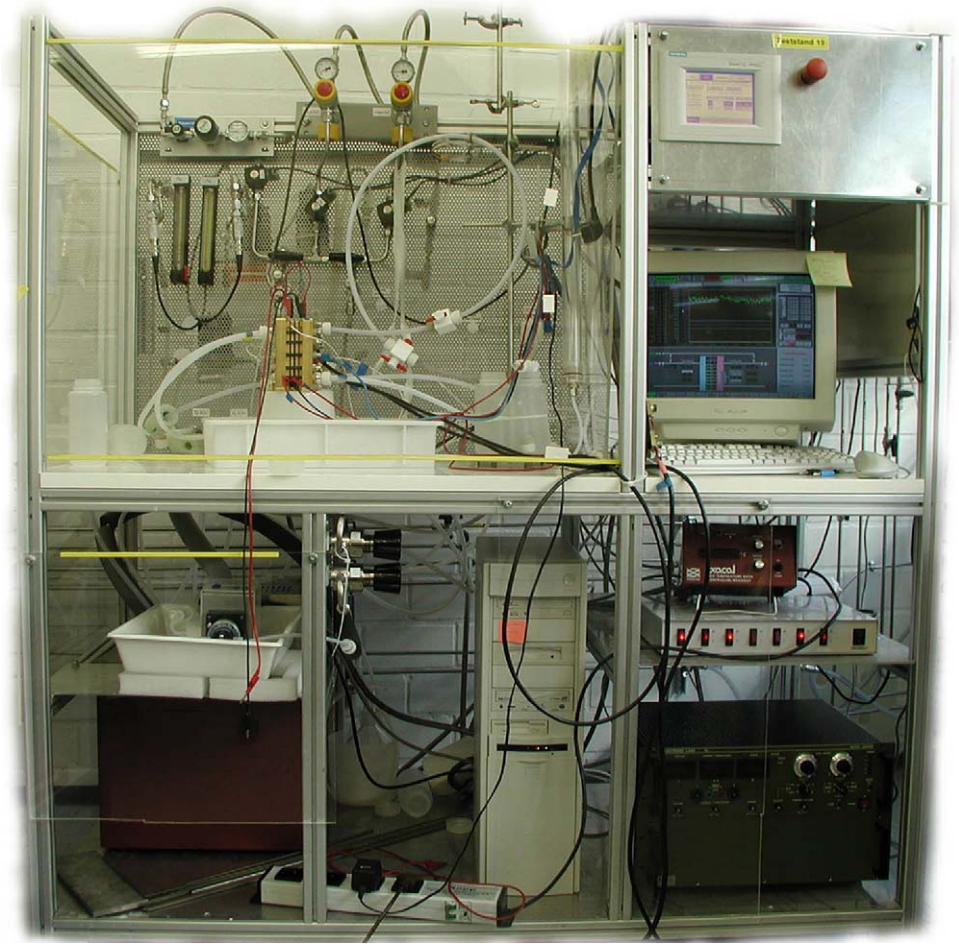

Fig. 4. Photo of the AFC test facility equipped with the three cell short stack.

Fig. 6(A) the *V–i* characteristics measured at various temperatures with nickel anodes and silver cathodes are displayed. In the diagram on the top the measured *V–i* characteristic are displayed. The electrolyte resistance was measured by current-interruption or by EIS in order to eliminate the influence of the electrolyte resistance on the measured *V–i* characteristics. The *V–i* characteristics corrected by the *iR* drop are displayed in Fig. 6(B).

An importance requirement of the stack is the operation at ambient pressure. So the dependence of the electrochemical performance as function of the pressures of the media was investigated. For this purpose the pressure of the anode and cathode media were varied individually. During the experiments the current density was kept constant at 80 mA cm^{-2}, the pressure of the invariable media was kept constant at 970 mbar and also the pressure of the electrolyte was kept constant at 1020 mbar.

The variation of the oxygen pressure does not strongly influence the electrochemical performance of the cell as shown in

Table 2
Resistance of the electrolyte-filled diaphragms, active area 50 cm^2, $T = 70\,^{\circ}C$

Material	Measured resistance (mΩ)	Specific resistance (Ωcm^2)	Specific resistance of diaphragm[a] (Ωcm^2)	Specific resistance of diaphragm thickness[b] (Ωcm)
Polyethylene plates, 3 mm	20.47	1.02	0.78	2.6
Celgard 3401 (on anode surface as well as on cathode surface), the distance between the electrodes was 1.5 mm	7.00	0.35	0.23	11.5
Non-woven polypropylene, 3 mm distance between the electrodes	5.15	0.26	0.09	0.3

[a] Additional resistance induced by the diaphragm, which increases the electrolyte resistance.
[b] Specific resistance of the diaphragm material.

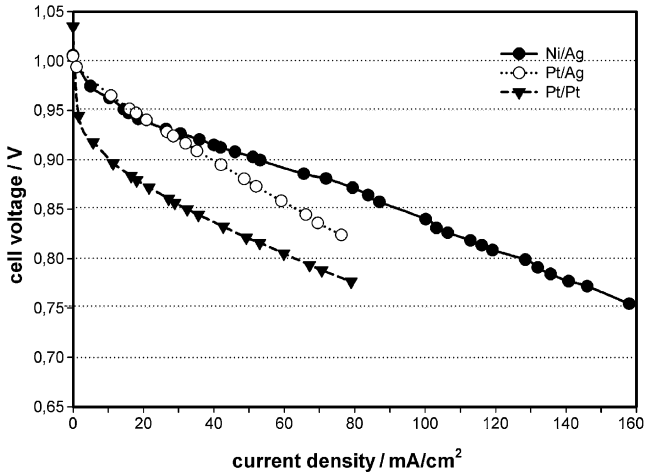

Fig. 5. *V–i* characteristics for various combinations of electrodes in alkaline fuel cells, operation conditions: $p_{oxygen} = 990$ mbar, $p_{hydrogen} = 980$ mbar, $p_{KOH} = 1000$ mbar, and $T = 70\,^{\circ}C$.

Fig. 7. The initial weak increase is induced by the increasing oxygen concentration in the cathode; over 1045 mbar the electrochemical performance decreases which is explained by increased penetration of the oxygen into the gas diffusion

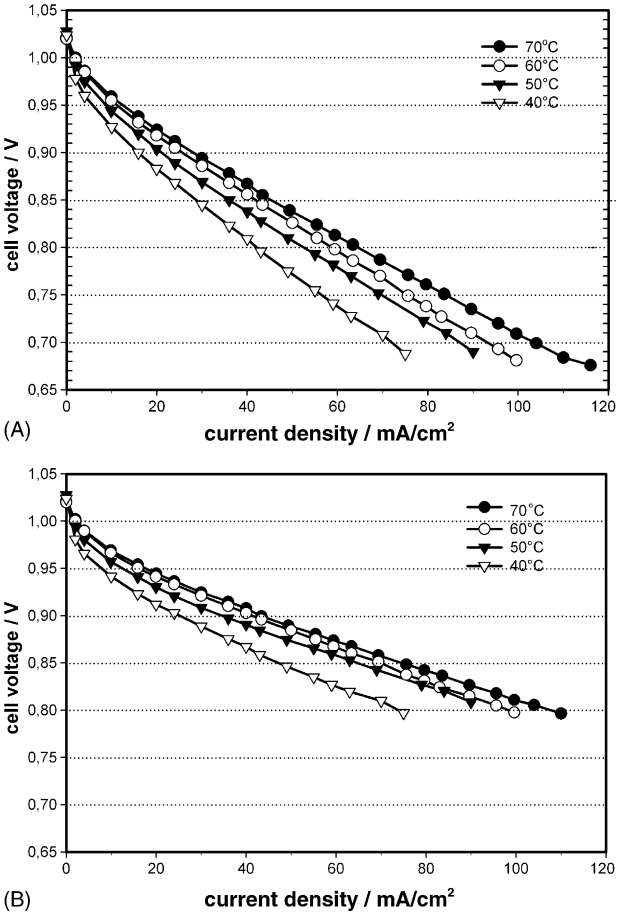

Fig. 6. *V–i* characteristics measured at various temperatures: (A) measured *V–i* characteristics; (B) *iR* drop corrected cell voltages, the operation combinations of the alkaline fuel cells are: $p_{oxygen} = 990$ mbar, $p_{hydrogen} = 980$ mbar, and $p_{KOH} = 1000$ mbar.

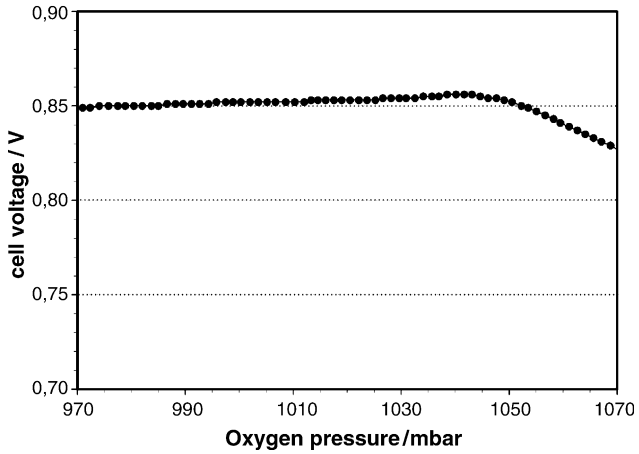

Fig. 7. Cell voltage at constant current density (80 mA cm^{-2}) as function of the oxygen pressure. The hydrogen pressure was kept constant at 970 mbar, the electrolyte pressure was kept constant at 1020 mbar; the cell was equipped the nickel anodes and silver cathodes. Electrolyte-filled Celgard 3401 membranes on both electrodes, the distance between the electrodes was 1.5 mm, $T = 70\,^{\circ}C$.

electrode and by displacement of the electrolyte out of the electrode. Therefore, three phase zone, in which the reaction takes place, decreases resulting in a decreased electrochemical performance.

The behavior of the cell voltage upon variation of the hydrogen pressure is similar (Fig. 8). Caused by the higher diffusion coefficient of hydrogen the decrease of the electrochemical performance starts already at 1005 mbar. For higher pressures the hydrogen penetrated the electrolyte which is obvious as hydrogen bubbles can be observed in the electrolyte outlet. As a consequence the ion conductivity decreases due to the bubbles, and more importantly also the cathode kinetics are influenced negatively. In particular, part of the oxygen will react directly with the hydrogen by a purely chemical path, which is a parallel reaction to the wanted fuel cell reaction. Therefore, the drop

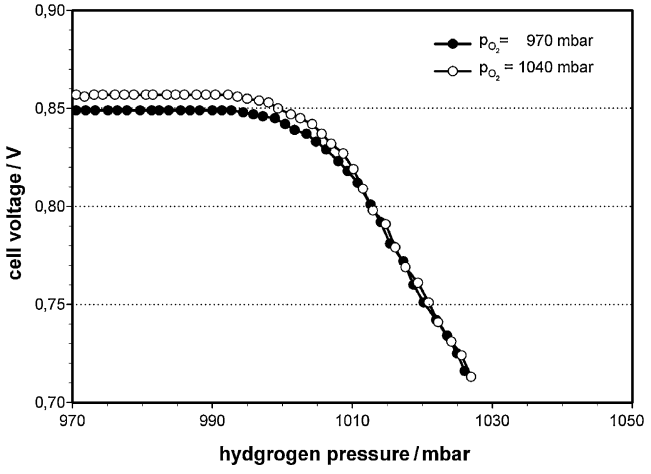

Fig. 8. Cell voltage at constant current density (80 mA cm^{-2}) as a function of the hydrogen pressure, the oxygen pressure was kept constant at 970 mbar (filled circles) and 1040 mbar (open circles). The electrolyte pressure was kept constant at 1020 mbar; the cell was equipped the nickel anodes and silver cathodes, Celgard 3401 membranes on both electrodes, the distance between the electrodes was 1.5 mm, $T = 70\,^{\circ}C$.

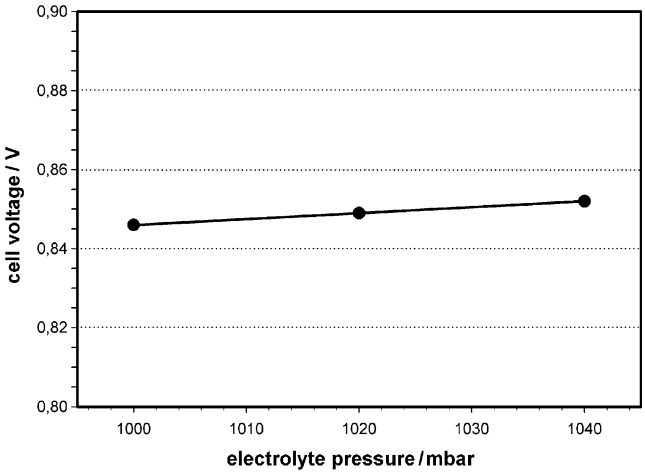

Fig. 9. Cell voltage at constant current density (80 mA cm^{-2}) as function of the electrolyte pressure, the oxygen pressure as well as the hydrogen pressure were kept constant at 970 mbar. The cell was equipped the nickel anodes and silver cathodes, Celgard 3401 membranes on both electrodes, the distance between the electrodes was 1.5 mm, $T = 70\,^{\circ}C$.

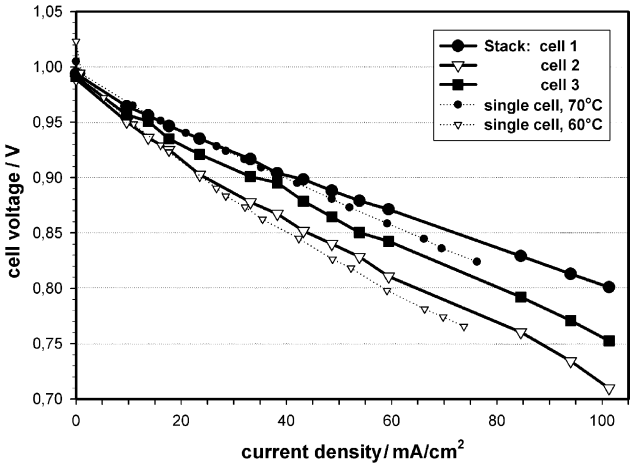

Fig. 10. *V–i* characteristics of the single cells in the three-cell stack, the oxygen pressure as well as the hydrogen pressure were kept constant at 970 mbar, the electrolyte pressure was kept constant at 1000 mbar, the set temperature was set to 70 °C. The temperature of the cell in the center was approximately 60 °C, the stack was equipped with platinum anodes and silver cathodes, electrolyte-filled non-woven polypropylene with an distance of 2 mm between the electrodes was used.

in the electrochemical performance with increasing hydrogen pressure is more significant than it is with increasing oxygen pressure.

An increased oxygen pressure at unchanged electrolyte pressure does not change the behavior of the cell as a function of the hydrogen pressure (open circles in Fig. 8) because the pressure differential between hydrogen and electrolyte is the important factor which affects the behavior.

The electrochemical performance during the variation of the electrolyte pressure is shown in Fig. 9. The electrolyte pressure could only be varied in a small pressure range, because at lower electrolyte pressures of approximately 30 mbar below the pressure of hydrogen the hydrogen diffuses into the electrolyte space as shown above. At higher electrolyte pressures the electrolyte penetrates further into the gas diffusion electrodes leading to increase active area. With increasing electrolyte pressure an improved electrochemical performance is observed.

The investigated dependence of the performance on the pressure of the media shows that stack performance cannot be improved significantly by increasing the pressures. Therefore the AFC stack is ideally suited for operation at ambient pressures.

In addition to the investigation of the behavior of the single cells, the stack concept was tested as three cell short stack. In Fig. 10 the individual cell voltages of the short stack are displayed. The stack is temperature controlled by heating both end plates. As a consequence the cell in the middle has a lower temperature of approximately 60 °C. In order to compare the cell voltages in the stack with the single cell performance, single cell results at 60 and 70 °C are added in the diagram. The difference in the cell voltages in the stack are mainly determined by the differences in the cell temperature. A loss of electrochemical performance in the stack compared with single cells is not observed in the short stack.

5. Conclusions

The stack, which was designed at the DLR, is able to operate at ambient pressures of the media as it was planned. Therefore, no overpressure is needed and consequently no energy-consuming compression of air. The construction principle of the stack demands a low pressure difference of the media. The sealing of the stack was very successful during the operation of the stack so far as no electrolyte leakage out of the stack was observed.

The *V–i* characteristics of the single cells and the cells in the short stack does not differ significantly. It can be concluded the loss of electrochemical performance will not be dramatic in a long stack. The difference of the performance of individual cell voltages in the stack are induced by temperature differences for the different cells and can be reduced by improving the thermal management or thermal isolation of the stack.

The stack can operate with various combinations of electrodes, whereupon the combination of gas diffusion electrodes with nickel catalysts as anodes and with silver catalysts as cathodes yield the best results. In addition, this combination uses cheaper electrodes than electrodes with platinum catalysts.

The designed stack demonstrates that an alkaline fuel cell stack can be realized in a bipolar design and it can be operated without overpressures.

References

[1] V. Plzak, H. Wendt, Brennstoffzellen, VDI Verlag, Düsseldorf, 1990.
[2] J. Nitsch, C.-J. Winter, Wasserstoff als Energieträger, Springer Verlag, Berlin, 1986.
[3] E. Gülzow, J. Power Sources 61 (1996) 99.
[4] K. Kordesch, G. Simader, Fuel Cells and their Applications, VCH-Verlag, Weinheim, 1996.

[5] E. Gülzow, M. Schulze, G. Steinhilber, K. Bolwin, Carbon dioxide tolerance of gas diffusion electrodes for alkaline fuel cells, in: Proceedings of the Fuel Cell Seminar, San Diego, 1994, p. 319.
[6] E. Gülzow, N. Wagner, M. Schulze, Fuel Cells 3 (2003) 67.
[7] D.P. Davies, P.L. Adcock, M. Turpin, S.J. Rowen, J. Appl. Electrochem. 30 (2000) 101.
[8] D.P. Davies, P.L. Adcock, M. Turpin, S.J. Rowen, J. Power Sources 86 (2000) 237.
[9] B. Mattsson, H. Ericson, L.M. Torell, F. Sundfolm, Electrochim. Acta 45 (2000) 1405.
[10] Hübner, E. Roduner, J. Mater. Chem. 9 (1999) 409.
[11] M. Schulze, M. Lorenz, N. Wagner, E. Gülzow, Fresenius J. Anal. Chem. 365 (1999) 106.
[12] F.N. Büchi, B. Gupta, O. Haas, G.G. Scherer, Electrochim. Acta 40 (1995) 345.
[13] E. Gülzow, A. Helmbold, T. Kaz, R. Reißner, M. Schulze, N. Wagner, G. Steinhilber, J. Power Sources 86 (2000) 352.
[14] S. Gupta, D. Tryk, S.K. Zecevic, W. Aldred, D. Guo, R.F. Savinell, J. Appl. Electrochem. 28 (1998) 673.
[15] E. Gülzow, M. Fischer, A. Helmbold, R. Reißner, M. Schulze, N. Wagner, M. Lorenz, B. Müller, T. Kaz, Innovative production technique for PEFC and DMFC electrodes and degradation of MEA-components, in: Proceedings of the Fuel Cell Seminar 1998, Palm Springs, 16–19 November, 1998, p. 469.
[16] E. Gülzow, T. Kaz, M. Lorenz, A. Schneider, M. Schulze, Degradation of PEFC components, in: Proceedings of the Fuel Cell Seminar, Portland, 30 October–2 November 2000, 2000, p. 156.
[17] M.S. Wilson, J.A. Valerio, S. Gottesfeld, Electrochim. Acta 40 (1995) 355.
[18] P.G. Dirven, W.J. Engelen, C.J.M. Van Der Poorten, J. Appl. Electrochem. 25 (1995) 122.
[19] E. Gülzow, M. Schulze, G. Steinhilber, J. Power Sources 106 (2002) 126.
[20] S. Gultekin, M.A. Al-Saheh, A.S. Al-Zakri, K.A.A. Abbas, Int. J. Hydrogen Energy 21 (1996) 485.
[21] Y. Kiros, S. Schwartz, J. Power Sources 87 (2000) 101.
[22] Sleem-Ur Rahman, M.A. Al-Saleh, A.S. Al-Zakri, S. Gultekin, J. Appl. Electrochem. 27 (1997) 215.
[23] M. Schulze, K. Bolwin, E. Gülzow, W. Schnurnberger, Fresenius J. Anal. Chem. 353 (1995) 778.
[24] E. Gülzow, et al., PTFE bonded gas diffusion electrodes for alkaline fuel cells, in: Proceedings of the Ninth World Hydrogen Energy Conference, Paris, 1992, p. 1507.
[25] A. Khalidi, B. Lafage, P. Taxil, G. Gave, M.J. Clifton, P. Cezac, Int. J. Hydrogen Energy 21 (1996) 25.
[26] M. Schulze, E. Gülzow, G. Steinhilber, Appl. Surf. Sci. 179 (2001) 252.
[27] N. Wagner, E. Gülzow, M. Schulze, W. Schnurnberger, in: H. Steeb, H. Aba Oud (Eds.), Gas Diffusion Electrodes for Alkaline Fuel Cells in Solar Hydrogen Energy, German–Saudi Joint Program on Solar Hydrogen Production and Utilization Phase II 1992–1995, Deutsches Zentrum fuer Luft- und Raumfahrt, Stuttgart, 1996. ISBN 3-89100-028-6.
[28] M. Schulze, E. Gülzow, J. Power Sources 127 (2004) 252.
[29] N. Wagner, M. Schulze, E. Gülzow, J. Power Sources 127 (2004) 264.
[30] E. Gülzow, M. Schulze, J. Power Sources 127 (2004) 243.